



ARTICLE

Acremotins A–D, peptaibiotics produced by the soil-derived fungus *Acremonium persicinum* SC0105

Chen Wang^{1,2} · Ping Wu¹ · Lei Yao¹ · Jinghua Xue¹ · Liangxiong Xu¹ · Hanxiang Li¹ · Wangqiu Deng³ · Xiaoyi Wei¹

Received: 22 May 2018 / Revised: 10 July 2018 / Accepted: 23 July 2018 / Published online: 8 August 2018

© The Author(s) under exclusive licence to the Japan Antibiotics Research Association 2018

Abstract

Four new peptaibiotics, acremotins A–D (**1–4**) featuring three α,α -dialkylated amino acid–imino acid motifs and an unreduced C-terminal residue, along with the known peptaibiotic XR586 (**5**) were isolated from the solid cultures of the soil-derived fungus *Acremonium persicinum* SC0105. Their primary structures were characterized by detailed analysis of the HRESIMS/MS fragmentation pattern combined with comprehensive interpretation of the 1D and 2D NMR spectroscopic data. The absolute configurations of amino acid residues were determined by the advanced Marfey's method. Sequence alignment result shows that **1–4** are closely related to zervamicin IIB and emerimicin IIA, thus belong to peptaibiotic subfamily-3 (SF3). The three-dimensional (3D) structure of **4** was established by theoretical conformational analysis using the *ab initio* density functional theory (DFT) method, which, together with the CD spectrum, indicated an amphiphilic and helical structure for **4**. **1–5** actively inhibited the growth of gram-positive bacterial pathogens, and amongst them **4** was the most potent compound showing MIC of 12.5 and 6.25 $\mu\text{g}/\text{ml}$ against *S. aureu* and MRSA strains, respectively. **1–5** were also cytotoxic against three human cancer cell lines with IC_{50} ranging from 1.2 to 21.6 μM .

Introduction

Membrane-active peptaibiotics are a group of fungal peptidic natural products known to establish voltage-dependent ion channels across lipid bilayer membrane [1–3], and consequently display a wide range of biological properties including antibacterial [4], antiviral [5, 6], antifungal [7, 8], and cytotoxic activities [9, 10]. The pore-forming ability of these non-ribosomally biosynthesized peptides is mainly derived from their amphipathic nature and unique amino

acid composition which features a high content of non-proteinogenic α,α -dialkylated amino acid residues such as 2-aminoisobutyric acid (Aib) and isovaline (Iva). The presence of these rare amino acids facilitates the formation of helical structures due to the steric constraints arising from the extra alkyl substituent at the α -carbon [11–14]. Apart from the frequent appearance of non-proteinogenic amino acid residues in the peptide sequence, other structural features like the *N*-acylated N-terminus and the C-terminal amino alcohol, amine, amide or sugar alcohol group also make peptaibiotics distinctive from other peptide antibiotics [15].

By virtue of the unusual structure, the superior biological activity and the unique mode of action, peptaibiotics have attracted intensive attention from both scientific community and pharmaceutical industry ever since the discovery of alamethicin, the prototype of peptaibiotics, from the biocontrol fungus *Trichoderma viride* [16]. To date, the sequences of over 1400 peptaibiotics are deposited in the Peptaibiotic Database (<http://peptaibiotics-database.boku.ac.at>) with most of which being peptaibols, while others falling into subgroups of cyclic peptaibiotics, lipoamino-peptides, lipopeptaibols, all-Aib-replaced peptides, and other peptaibiotics. A majority of the naturally occurring peptaibiotics are discovered in the fungal species of genus

Electronic supplementary material The online version of this article (<https://doi.org/10.1038/s41429-018-0086-3>) contains supplementary material, which is available to authorized users.

✉ Ping Wu
wuping@scbg.ac.cn

¹ Key Laboratory of Plant Resources Conservation and Sustainable Utilization, South China Botanical Garden, Chinese Academy of Sciences, Guangzhou 510650, People's Republic of China

² University of Chinese Academy of Sciences, Yuquanlu 19A, Beijing 100049, People's Republic of China

³ State Key Laboratory of Applied Microbiology Southern China, Guangdong Institute of Microbiology, Guangzhou 510070, People's Republic of China

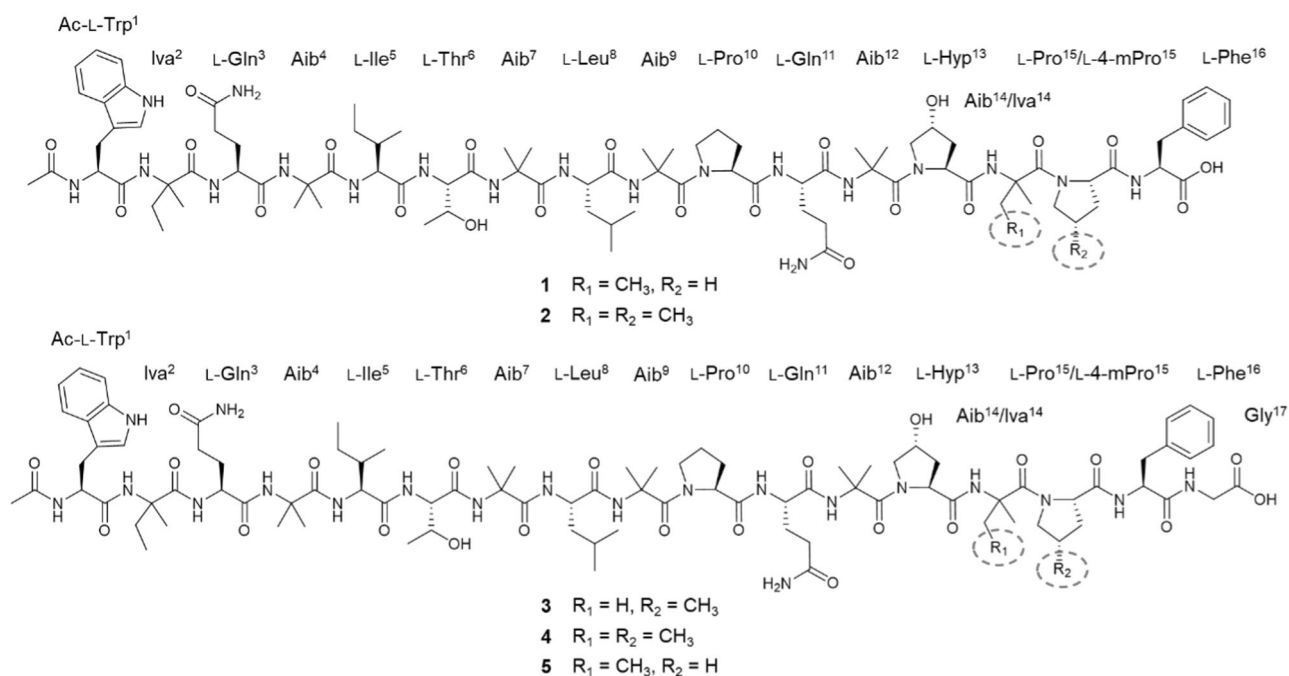


Fig. 1 Structures of acremotins A–D (1–4) and XR586 (5)

Trichoderma [17], while many other filamentous fungi, like species of genus *Acremonium* also produce a variety of peptaibiotics [18–24].

In our previous chemical investigation on the soil-derived filamentous fungus *Acremonium persicinum* SC0105, a group of dimeric aremines, bisacremines A–G, featuring a unique carbon skeleton, were obtained [25, 26]. As a continuing effort to explore the secondary metabolites produced by this strain, five peptaibiotics (1–5) (Fig. 1), featuring three α,α -dialkylated amino acid (Aib/Iva)–imino acid [Pro/4-hydroxyproline (Hyp)/4-methylproline (4-mPro)] motifs and an unreduced C-terminal residue, were isolated and their structures were characterized by extensive analysis of the HRESIMS/MS and NMR spectroscopic data. Moreover, the 3D structure of 4 was established by theoretical conformational analysis using the *ab initio* density functional theory (DFT) method. Herein, we describe the isolation, structure elucidation, and bioactivity of these peptaibiotics.

Results and discussion

Structure elucidation

The solid cultures of *A. persicinum* SC0105 were extracted with 95% aqueous ethanol and the solution was dried under vacuum. The resulting residue was separated and purified using Diaion HP-20 resin and ODS column

chromatography as well as preparative HPLC to afford compounds 1–5. Although the ^1H and ^{13}C NMR spectra in CD_3OH (with or without a few drops of CF_3COOH , Table 1) of 1–5 appeared perplexing upon first glance, the peptidic nature of these compounds was successfully revealed by the presence of multiple amidic proton signals at δ_{H} 7.4–8.5 and carbonyl carbon signals at δ_{C} 170–180. ^1H NMR spectra of these peptides all displayed characteristic methyl singlets at δ_{H} 1.3–1.7 and one sharp methyl singlet at δ_{H} 2.04, while the ^{13}C NMR spectra exhibited diagnostic quaternary carbon resonances at δ_{C} 56–61 indicating that 1–5 are α,α -dialkylated amino acid containing peptaibiotics with acetylated N-termini. The observation of fourteen aromatic carbon signals at δ_{C} 110–140 in the ^{13}C NMR spectra and one down-field broad indolic NH proton signal at δ_{H} 10.41 in the ^1H NMR spectra of 1–5 suggested the incorporation of two aromatic amino acid residues in their peptide sequences and one of which is tryptophan. The similarity of 1D NMR spectra between peptaibiotics 1–5 along with their closely related HRESIMS determined molecular weight suggest that they are structural analogues to each other which only differ in one or two amino acid residues in the primary structures. With the aforementioned structural information in hand, the amino acid composition and the complete sequence of each peptaibiotic were subsequently investigated by detailed analysis of the HRESIMS/MS and 2D NMR spectroscopic data.

The positive mode HRESIMS full-scan spectrum of acremotin A (1) displayed an $[\text{M} + \text{Na}]^+$ pseudomolecular

Table 1 ^1H (600 MHz) and ^{13}C (150 MHz) NMR Data (CD_3OH^a , δ in ppm) of Acremotins A–D (**1–4**)

Position	1		2		3		4	
	δ_{C} , type	δ_{H} m (<i>J</i> in Hz)	δ_{C} , type	δ_{H} m (<i>J</i> in Hz)	δ_{C} , type	δ_{H} m (<i>J</i> in Hz)	δ_{C} , type	δ_{H} m (<i>J</i> in Hz)
<i>Ac</i>								
C=O	174.4, C		174.3, C		174.6, C		174.5, C	
CH ₃	22.5 ^b , CH ₃	2.04 s	22.3, CH ₃	2.04 s	22.6 ^b , CH ₃	2.04 s	22.6 ^b , CH ₃	2.04 s
<i>Trp</i> ¹								
NH		8.31 d (4.3)		8.30 d (4.3)		8.34 d (5.0)		8.32 d (3.5)
C=O	174.66 ^c , C		174.7, C		174.66 ^c , C		174.69 ^c , C	
α	57.5, CH	4.56 m	57.4, CH	4.56 m	57.5, CH	4.58 m	57.5, CH	4.57 m
β	28.3, CH ₂	3.30 m, 3.15 m	28.3, CH ₂	3.29 m, 3.15 m	28.3, CH ₂	3.30 m, 3.16 m	28.3, CH ₂	3.30 m, 3.16 m
1'-NH		10.41, brs		10.41 brs		10.41 brs		10.41, brs
2'	124.3, CH	7.18 brs	124.3, CH	7.18 brs	124.5, CH	7.18 brs	124.4, CH	7.18 brs
3'	110.6, C		110.6, C		110.6, C		110.6, C	
4'	128.3, C		128.3, C		128.3, C		128.3, C	
5'	118.9, CH	7.56 d (8.1)	119.0, CH	7.57 d (7.5)	119.0, CH	7.56 d (7.7)	119.0, CH	7.56 d (7.5)
6'	119.7, CH	7.01 t (7.5)	119.8, CH	7.01 t (7.5)	119.9, CH	7.01 t (7.6)	119.8, CH	7.01 t (7.5)
7'	122.5, CH	7.10 t (7.5)	122.5, CH	7.10 t (7.5)	122.6, CH	7.10 t (7.6)	122.6, CH	7.10 t (7.5)
8'	112.5, CH	7.31–7.37 ^b m	112.4, CH	7.31–7.37 ^b m	112.6, CH	7.31–7.37 ^b m	112.5, CH	7.31–7.37 ^b m
9'	138.2, C		138.2, C		138.3, C		138.2, C	
<i>Iva</i> ²								
NH		8.33 s		8.31 s		8.31 s		8.35 s
C=O	178.9, C		178.9, C		179.0, C		179.0, C	
α	60.3, C		60.3, C		60.4, C		60.4, C	
α -CH ₃	22.5, CH ₃	1.33 s	22.5 ^b , CH ₃	1.33 s	22.6 ^b , CH ₃	1.33 s	22.6 ^b , CH ₃	1.33 s
β	27.88 ^c , CH ₂	2.07–2.17 ^b m, 1.69 m	27.88 ^c , CH ₂	2.09–2.19 ^b m, 1.69 m	27.9, CH ₂	2.08–2.18 ^b m, 1.70 m	27.86 ^c , CH ₂	2.08–2.18 ^b m, 1.70 m
γ	7.7, CH ₃	0.82 t (7.5)	7.7, CH ₃	0.82 t (7.5)	7.6, CH ₃	0.82 t (7.5)	7.7, CH ₃	0.82 t (7.5)
<i>Gln</i> ³								
NH		8.27 d (4.8)		8.28 d (4.9)		8.29 d (4.9)		8.29 d (5.0)
C=O	174.8, C		174.8 ^b , C		174.8, C		174.8, C	
α	58.4, CH	3.97 m	58.4, CH	3.97 m	58.4, CH	3.96 m	58.4, CH	3.96 m
β	26.9, CH ₂	2.07–2.17 ^b m, 1.90–2.00 ^b m	26.9, CH ₂	2.09–2.19 ^b m, 1.91–2.01 ^b m	26.9, CH ₂	2.08–2.18 ^b m, 1.91–2.00 ^b m	26.9, CH ₂	2.08–2.18 ^b m, 1.90–2.00 ^b m
γ	32.8, CH ₂	2.27–2.50 ^b m	32.8, CH ₂	2.29–2.51 ^b m	32.8, CH ₂	2.29–2.51 ^b m	32.8, CH ₂	2.28–2.51 ^b m
δ	177.3, C		177.3, C		177.6, C		177.4, C	
δ -NH ₂		7.57 d (8.1), 6.79 brs		7.57 d (8.1), 6.79 brs		7.57 d (8.1), 6.79 brs		7.57 d (7.4), 6.79 brs
<i>Aib</i> ⁴								
NH		8.09 s		8.09 s		8.08 s		8.09 s
C=O	177.9, C		177.9, C		177.87 ^{b,c} , C		177.9, C	
α	57.6, C		57.6, C		57.6, C		57.6, C	
α -CH ₃	27.11 ^c , CH ₃	1.46 s	27.2, CH ₃	1.46 s	27.2 ^b , CH ₃	1.46 s	27.2 ^b , CH ₃	1.46 s
β	23.3, CH ₃	1.39 s	23.2, CH ₃	1.39 s	23.24 ^b , CH ₃	1.39 s	23.2, CH ₃	1.39 s
<i>Ile</i> ⁵								
NH		7.80 d (5.2)		7.79 d (5.7)		7.80 d (5.7)		7.80 d (5.7)
C=O	175.9, C		175.9, C		175.78 ^c , C		176.0, C	
α	62.4, CH	3.80 m	62.39 ^c , CH	3.81 m	62.2, CH	3.80 m	62.4, CH	3.80 m

Table 1 (continued)

Position	1		2		3		4	
	δ_C , type	δ_H m (J in Hz)	δ_C , type	δ_H m (J in Hz)	δ_C , type	δ_H m (J in Hz)	δ_C , type	δ_H m (J in Hz)
β	36.3, CH	1.90–2.00 ^b m	36.3, CH	1.91–2.01 ^b m	36.4, CH	1.90–2.00 ^b m	36.4, CH	1.90–2.00 ^b m
β -CH ₃	15.8, CH ₃	0.91 d (6.6)	15.8, CH ₃	0.91 d (7.2)	15.8, CH ₃	0.91 d (7.0)	15.8, CH ₃	0.91 d (7.5)
γ	27.13 ^c , CH ₂	1.59 m, 1.24 m	27.1, CH ₂	1.59 m, 1.24 m	27.2 ^b , CH ₂	1.59 m, 1.24 m	27.2 ^b , CH ₂	1.59 m, 1.24 m
δ	10.6, CH ₃	0.80 t (7.2)	10.6, CH ₃	0.80 t (7.5)	10.6, CH ₃	0.80 t (7.5)	10.6, CH ₃	0.80 t (7.5)
<i>Thr</i> ⁶								
NH		7.76 d (4.7)		7.76, d (4.7)		7.77 d (4.7)		7.76 d (4.4)
C=O	173.5, C		173.4, C		173.5, C		173.5, C	
α	66.0, CH	3.73 m	66.0, CH	3.76 m	66.0, CH	3.77 m	66.0, CH	3.78 m
β	67.2, CH	4.20–4.29 ^b m	67.2, CH	4.20–4.29 ^b m	67.3, CH	4.20–4.31 ^b m	67.2, CH	4.20–4.29 ^b m
γ	20.1, CH ₃	1.23 d (6.3)	20.2, CH ₃	1.24 d (6.2)	20.1, CH ₃	1.23 d (6.3)	20.1, CH ₃	1.23 d (6.2)
<i>Aib</i> ⁷								
NH		7.87 s		7.87 s		7.88 s		7.88 s
C=O	177.7 ^b , C		177.7 ^b , C		177.92 ^{b,c} , C		177.8 ^b , C	
α	58.0, C		57.9, C		58.00 ^c , C		58.0, C	
α -CH ₃	26.4 ^b , CH ₃	1.53 ^b s	26.5, CH ₃	1.53 ^b s	26.5, CH ₃	1.53 ^b s	26.5, CH ₃	1.53 ^b s
β	27.7, CH ₃	1.50 s	27.7, CH ₃	1.50 s	27.7, CH ₃	1.50 s	27.7, CH ₃	1.50 s
<i>Leu</i> ⁸								
NH		7.47 d (7.3)		7.46 d (7.3)		7.48 d (7.2)		7.47 d (7.2)
C=O	175.55 ^{b,c} , C		175.5 ^b , C		175.2, C		175.2, C	
α	54.5, CH	4.20–4.29 ^b m	54.5, CH	4.20–4.29 ^b m	54.6, CH	4.20–4.29 ^b m	56.7, CH	4.20–4.29 ^b m
β	41.6, CH ₂	1.79–1.88 ^b m	41.6, CH ₂	1.80–1.90 ^b m	41.7, CH ₂	1.80–2.00 ^b m	41.6, CH ₂	1.80–1.89 ^b m
γ	25.7, CH	1.79–1.88 ^b m	25.7, CH	1.80–1.90 ^b m	25.7 ^b , CH	1.80–2.00 ^b m	25.7, CH	1.80–1.89 ^b m
γ -CH ₃	21.4, CH ₃	0.87 d (6.4)	21.4, CH ₃	0.87 d (6.4)	21.4, CH ₃	0.89 d (6.4)	21.4, CH ₃	0.88 d (6.4)
δ	23.23 ^c , CH ₃	0.91 d (6.4)	23.3, CH ₃	0.91 d (6.3)	23.6, CH ₃	0.93 d (6.4)	23.29 ^c , CH ₃	0.93 d (6.4)
<i>Aib</i> ⁹								
NH		8.14 s		8.14 s		8.14 s		8.15 s
C=O	175.55 ^{b,c} , C		175.5 ^b , C		175.7, C		175.7 ^b , C	
α	57.8, C		58.0, C		57.9, C		57.9, C	
α -CH ₃	26.4 ^b , CH ₃	1.53 ^b s	26.4, CH ₃	1.53 ^b s	26.4 ^b , CH ₃	1.53 ^b s	26.4, CH ₃	1.53 ^b s
β	23.6, CH ₃	1.61 ^b s	23.6, CH ₃	1.61 ^b s	23.2, CH ₃	1.62 s	23.6, CH ₃	1.61 s
<i>Pro</i> ¹⁰								
C=O	175.1, C		175.1, C		175.3, C		175.3, C	
α	64.3, CH	4.34 m	64.3, CH	4.35 m	64.4, CH	4.37 m	64.3, CH	4.36 m
β	30.0, CH ₂	2.27–2.51 ^b m, 1.79–1.88 ^b m	30.0, CH ₂	2.29–2.51 ^b m, 1.80–1.90 ^b m	30.0, CH ₂	2.29–2.51 ^b m, 1.80–2.00 ^b m	30.0, CH ₂	2.28–2.51 ^b m, 1.80–1.90 ^b m
γ	26.8, CH ₂	2.03 ^b m, 1.90–2.00 ^b m	26.8, CH ₂	2.03 ^b m, 1.91–2.01 ^b m	26.4 ^b , CH ₂	2.03 ^b m, 1.91–2.00 ^b m	26.8, CH ₂	2.03 ^b m, 1.91–2.00 ^b m
δ	50.4, CH ₂	3.91–4.04 ^b m, 3.69 m	50.4, CH ₂	4.00 m, 3.69 m	50.5, CH ₂	3.92–4.07 ^b m, 3.68 m	50.4, CH ₂	3.95–4.05 ^b m, 3.69 m
<i>Gln</i> ¹¹								
NH		8.20 d (8.5)		8.21 d (8.4)		8.21 d (8.5)		8.21 d (8.4)
C=O	173.6, C		173.7, C		173.9, C		173.8, C	
α	54.4, CH	4.35 m	54.5, CH	4.36 m	54.7, CH	4.37 m	54.5, CH	4.43 t (8.1)
β	27.82 ^c , CH	2.07–2.17 ^b m	27.84 ^c , CH	2.09–2.18 ^b m	28.0, CH	2.09–2.18 ^b m	27.90 ^c , CH	2.08–2.19 ^b m
γ	32.9, CH ₂	2.27–2.51 ^b m,	32.9, CH ₂	2.29–2.51 ^b m	33.0, CH ₂	2.29–2.51 ^b m	33.0, CH ₂	2.28–2.51 ^b m

Table 1 (continued)

Position	1		2		3		4	
	δ_C , type	δ_H m (J in Hz)	δ_C , type	δ_H m (J in Hz)	δ_C , type	δ_H m (J in Hz)	δ_C , type	δ_H m (J in Hz)
δ	177.7 ^b , C		177.7 ^b , C		177.87 ^{b,c} , C		177.8 ^b , C	
δ -NH ₂		7.63 brs, 6.88 brs		7.64 brs, 6.89 brs		7.64 d (8.1), 6.89 brs		7.63 brs, 6.88 brs
<i>Aib</i> ¹²								
NH		7.85 s		7.85 s		7.87 s		7.88 s
C=O	174.73 ^c , C		174.8 ^b , C		174.9, C		174.9, C	
α	57.9, C		57.8, C		57.7, C		58.1, C	
α -CH ₃	23.16 ^c , CH ₃	1.51 ^b s	23.2, CH ₃	1.51 ^b s	23.24 ^b , CH ₃	1.52 ^b s	23.25 ^c , CH ₃	1.52 ^b s
β	24.8, CH ₃	1.61 ^b s	24.8, CH ₃	1.61 ^b s	24.8, CH ₃	1.63 s	24.8, CH ₃	1.62 s
<i>Hyp</i> ¹³								
C=O	175.54 ^c , C		174.5 ^b , C		175.78 ^{b,c} , C		175.7 ^b , C	
α	62.2, CH	4.75 m	62.35 ^c , CH	4.76 m	62.5, CH	4.79 m	62.3, CH	4.79 m
β	38.3, CH ₂	2.27–2.51 ^b m, 1.79–1.88 ^b m	38.6, CH ₂	2.29–2.51 ^b m, 1.80–1.90 ^b m	38.4, CH ₂	2.29–2.51 ^b m, 1.80–2.00 ^b m	38.5, CH ₂	2.28–2.51 ^b m, 1.80–1.90 ^b m
γ	71.3, CH	4.40 ^b m	71.4, CH	4.41 ^b m	71.4, CH	4.40 ^b m	71.4, CH	4.40 ^b m
δ	58.2, CH ₂	3.87 d (12.5), 3.49 d (12.5)	58.2, CH ₂	3.87 d (12.5), 3.53 d (12.5)	58.1, CH ₂	3.88 d (12.5), 3.52 d (12.5)	58.2, CH ₂	3.88 d (12.5), 3.52 d (12.5)
<i>Iva</i> ¹⁴ / <i>Aib</i> ¹⁴								
NH		8.09 s		8.09 s		8.14 s		8.00 s
C=O	177.7 ^b , C		177.7 ^b , C		177.96 ^c , C		177.8 ^b , C	
α	61.43 ^c , C		61.3, C		57.98 ^c , C		61.5, C	
α -CH ₃	22.7, CH ₃	1.46 s	22.5 ^b , CH ₃	1.47 s	24.1, CH ₃	1.62 ^b s	22.0, CH ₃	1.46 s
β	29.7, CH ₂	1.90–2.00 ^b m	30.2, CH ₂	1.91–2.01 ^b m	25.7 ^b , CH ₃	1.51 ^b s	29.8, CH ₂	1.90–2.00 ^b m
γ	8.5, CH ₃	0.91 t (7.3)	8.7, CH ₃	0.91 t (7.2)			8.7, CH ₃	0.95 t (7.4)
<i>Pro15/4-mPro</i> ¹⁵								
C=O	175.54 ^{b,c} , C		175.5 ^b , C		175.98 ^c , C		175.7 ^b , C	
α	61.42 ^c , CH	4.25 ^b m	63.8, CH	4.25 ^b m	64.7, CH	4.28 m	64.7, CH	4.25 m
β	37.6, CH ₂	2.27–2.51 ^b m, 2.07–2.17 ^b m	38.2, CH ₂	2.29–2.51 ^b m, 1.80–1.90 ^b m	37.8, CH ₂	2.29–2.51 ^b m, 2.09–2.19 ^b m	37.8, CH ₂	2.28–2.51 ^b m, 2.08–2.19 ^b m
γ	26.1, CH ₂	2.03 ^b m, 1.90–2.00 ^b m	35.3, CH	1.91–2.01 ^b m	35.2, CH	2.09–2.19 ^b m	35.3, CH	2.08–2.19 ^b m
γ -CH ₃			16.2, CH ₃	0.95 d (5.9)	16.3, CH ₃	0.99 d (5.2)	16.3, CH ₃	0.98 d (5.9)
δ	49.9, CH ₂	3.82–3.90 ^b m, 3.63–3.73 ^b m	56.6, CH ₂	4.04 m, 3.21–3.27 ^b m	56.8, CH ₂	3.92–4.07 ^b m, 3.34–3.42 ^b m	49.9, CH ₂	3.95–4.05 ^b m, 3.34 m
<i>Phe</i> ¹⁶								
NH		8.09 ^b m		7.98 m		8.10 m		8.10 ^b m
C=O	174.5, C		174.5 ^b , C		174.7, C		174.71 ^c , C	
α	55.3, CH	4.52–4.61 ^b m	55.2, CH	4.55–4.61 ^b m	56.1, CH	4.50 m	56.1, CH	4.51 m
β	38.4, CH ₂	3.26–3.35 ^b m, 3.05 m	38.4, CH ₂	3.30 m, 3.05 m	37.6, CH ₂	3.34–3.42 ^b m, 3.08 m	37.5, CH ₂	3.39 m, 3.05 m
2', 6'	130.4, CH	7.31–7.37 ^b m	130.6, CH	7.31–7.37 ^b m	130.4, CH	7.31–7.37 ^b m	130.4, CH	7.31–7.37 ^b m
3', 5'	129.2, CH	7.29 t (7.0)	129.5, CH	7.31–7.37 ^b m	129.6, CH	7.31–7.37 ^b m	129.6, CH	7.31–7.37 ^b m
4'	127.2, CH	7.15 m	127.2, CH	7.17 m	127.5, CH	7.15–7.20 ^b m	127.5, CH	7.15–7.20 ^b m
<i>Gly</i> ¹⁷								
NH						7.78 m		7.79 ^b , m
C=O					171.3, C		171.2, C	

Table 1 (continued)

Position	1		2		3		4	
	δ_C , type	δ_H m (J in Hz)	δ_C , type	δ_H m (J in Hz)	δ_C , type	δ_H m (J in Hz)	δ_C , type	δ_H m (J in Hz)
α					42.0, CH ₂	3.92–4.07 ^b m	42.1, CH ₂	3.96–4.05 ^b m

^aFor **3** and **4**, a few drops of CF₃COOH were added

^bOverlapping signals

^cAssignments might be interchangeable within the same column

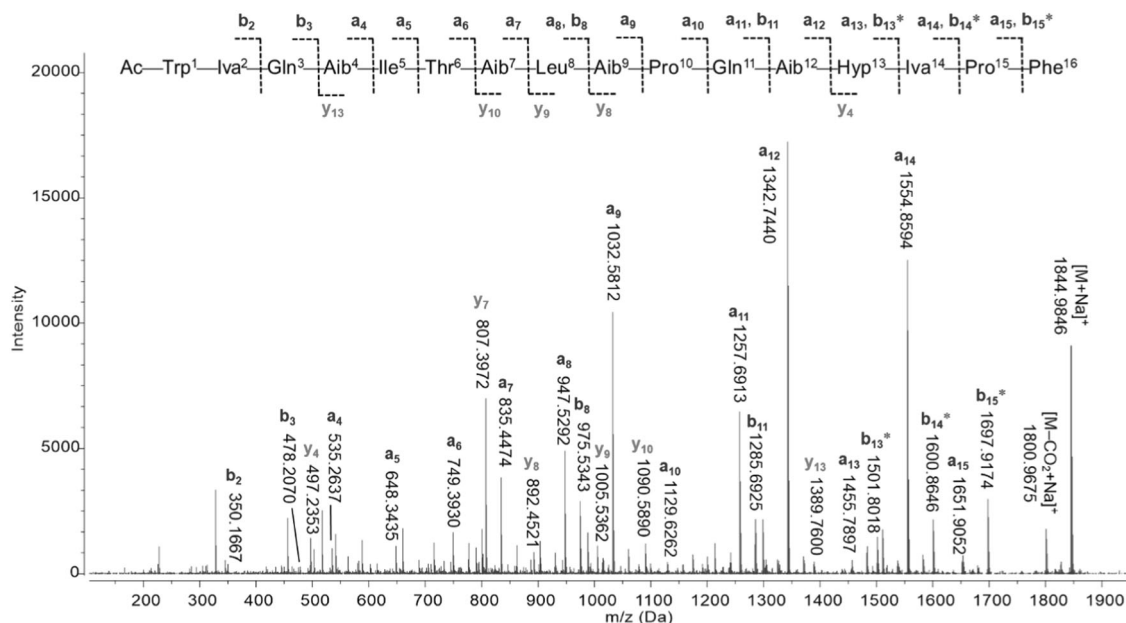


Fig. 2 HRESIMS/MS fragmentation pattern of the $[M + Na]^+$ ion of **1**. a_n , b_n , b_n^* and y_n represent $[a_n + Na - H]^+$, $[b_n + Na - H]^+$, $[b_n + Na + OH]^+$ and $[y_n + Na + H]^+$ daughter ions, respectively

ion at m/z 1844.9846 (calcd for C₈₉H₁₃₅N₁₉O₂₂Na), indicating a molecular formula of C₈₉H₁₃₅N₁₉O₂₂. Subsequent fragmentation of this sodium adduct using collision-induced dissociation (CID) was carried out to decipher the complete sequence of **1**. Unlike the fragmentation of protonated peptidic molecules which preferentially gives rise to b-type ions, cleavage of sodium-cationized peptides usually generates a mixture of sodiated a-, b- and y-type ions ($[a_n + Na - H]^+$, $[b_n + Na - H]^+$, $[b_n + Na + OH]^+$, $[y_n + Na + H]^+$, etc.) [27–29]. Indeed, fragmentation of the $[M + Na]^+$ ion of **1** produced four intense sodiated a-/y- type daughter ions at m/z 807.3972 ($[y_9 + Na + H]^+$), 1032.5812 ($[a_9 + Na - H]^+$), 1342.7440 ($[a_{12} + Na - H]^+$) and 1554.8594 ($[a_{14} + Na - H]^+$) (Fig. 2), arising from the cleavage of three labile peptide bonds between Aib/Iva and Pro/Hyp/4-mPro. Further examination of the fragmentation profile led to the identification of some less abundant sodiated a-, b- and y-ions. The appearance of a series of $[a_n + Na - H]^+$ ions at m/z 1651.9052, 1554.8594, 1455.7897, 1342.7440, 1257.6913, 1129.6262, 1032.5812, 947.5292, 835.4474,

749.3930, 648.3435, and 535.2637 (Fig. 2) corresponded to the consecutive loss of Phe¹⁶, Pro¹⁵, Val¹⁴/Iva¹⁴, Hyp¹³, Aib¹², Gln¹¹, Pro¹⁰, Aib⁹, Leu⁸/Ile⁸, Aib⁷, Thr⁶, and Leu⁵/Ile⁵ from the C-terminus of the $[M + Na]^+$ ion. Together with the presence of $[b_3 + Na - H]^+$ and $[b_2 + Na - H]^+$ ions at m/z 478.2070 and 350.1667, respectively, the C-terminal partial sequence of **1** was proposed as Gln³–Aib⁴–Leu⁵/Ile⁵–Thr⁶–Aib⁷–Leu⁸/Ile⁸–Aib⁹–Pro¹⁰–Gln¹¹–Aib¹²–Hyp¹³–Val¹⁴/Iva¹⁴–Pro¹⁵–Phe¹⁶. Excluding the mass of the acetyl group and the tryptophan residue from the $[b_2 + Na - H]^+$ ion gave an m/z around 121, suggesting the one remaining residue is either Val or Iva. The precise order of the Trp and Val/Iva residues, however, were unclear at that point due to the lack of fragmentation information provided by corresponding daughter ion peaks.

Next, the comprehensive interpretation of 2D NMR spectra, including ¹H-¹H COSY, TOCSY, HSQC, HMBC, and ROSEY, were carried out in order to identify the remaining N-terminal sequence as well as to distinguish the isomeric amino acid residues, such as Val/Iva and Leu/Ile.

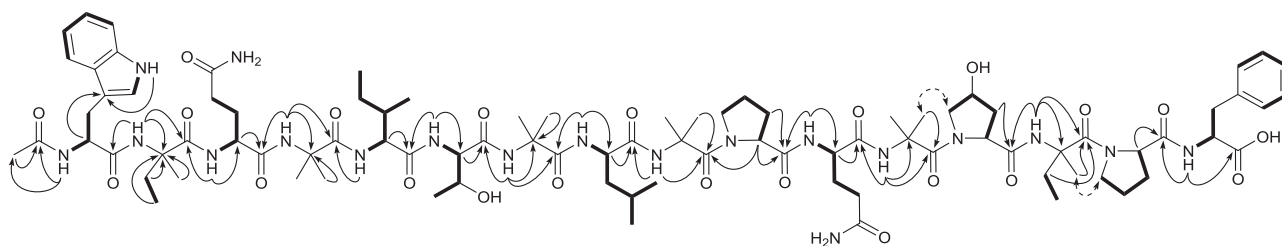


Fig. 3 Selected ^1H - ^1H COSY/TOCSY (bold lines), HMBC (plain arrows), and ROSEY (dashed arrows) correlations of **1**

^1H - ^1H COSY and TOCSY correlations observed for the NH, α -H and side chain protons established the spin systems of individual amino acid residues, while the assignments of ^1H and ^{13}C NMR chemical shifts for each residue were complemented by HSQC and HMBC experiments (Fig. 3). The HMBC correlations of the acetyl methyl protons at δ_{H} 2.04 and the amidic proton of Trp at δ_{H} 8.31 with the acetyl carbonyl carbon at δ_{C} 174.4 as well as the correlation of the amidic proton of Trp with the acetyl methyl carbon at δ_{C} 22.5 confirmed the peptide chain of **1** is initiated by an *N*-acetylated Trp at the N-terminus. The residue immediately adjacent to the *N*-acetylated Trp¹ was elucidated as isovaline based on the HMBC correlations of its amidic proton (δ_{H} 8.33, s) with the carbonyl carbon of Trp¹ (δ_{C} 174.7) and a quaternary α -carbon (δ_{C} 60.3), and the correlations of two sets of CH₃ protons (δ_{H} 1.33, s; δ_{H} 0.82, t) and one set of CH₂ protons (δ_{H} 2.14, m and 1.69, m) with this α -carbon (Fig. 3). Subsequently, the 5th, 8th and 14th residues were verified as Ile⁵, Leu⁸ and Iva¹⁴, respectively, in a similar manner. The HMBC correlations of the NH and α -H with neighboring amidic carbonyl carbons through $^2J_{\text{CH}}$ and $^3J_{\text{CH}}$ couplings together with ROSEY interactions between side chain protons of adjacent amino acid residues supported the primary structure of acremotin A (**1**) as Ac-Trp¹-Iva²-Gln³-Aib⁴-Ile⁵-Thr⁶-Aib⁷-Leu⁸-Aib⁹-Pr-Pro¹⁰-Gln¹¹-Aib¹²-Hyp¹³-Iva¹⁴-Pro¹⁵-Phe¹⁶.

The molecular formula of acremotin B (**2**) was established as C₉₀H₁₃₇N₁₉O₂₂ based on the [M + Na]⁺ ion peak found at m/z 1859.0042 (calcd for C₉₀H₁₃₇N₁₉O₂₂Na) in the positive mode HRESIMS full-scan spectrum. Consequently, the molecular weight of **2** is 14 amu higher than that of **1**, indicating the presence of an extra methyl substituent on one of the amino acid residues of **2**. The fragmentation of the sodium adduct ion produced a series of sodiated a-, b- and y- type daughter ions which were almost identical to those of **1** (Table S1, Supplementary Information), while a mass difference of 14 amu was observed between the [b₁₅ + Na + OH]⁺ ions of compounds **2** and **1**, suggesting an exchange of Pro¹⁵ in **1** with a methylproline (mPro) residue in **2**. Apart from the presence of resonance signals corresponding to an additional methyl group (δ_{H} 0.95; δ_{C} 16.2), the ^1H and ^{13}C NMR spectra of **2** were nearly superimposable to those of **1**. The extra methyl functionality is

attached to the γ -C of Pro¹⁵ as demonstrated by the TOCSY correlations of the protons within the spin system of this residue, and the HMBC interactions of the CH₃ protons (δ_{H} 0.95) with the β -, γ - and δ -carbons (δ_{C} 38.2, 35.3 and 56.6, respectively) through $^2J_{\text{CH}}$ and $^3J_{\text{CH}}$ couplings (Figure S1, Supplementary Information). Comprehensive interpretations of HSQC, HMBC, ^1H - ^1H COSY, TOCSY-HSQC, and ROSEY NMR spectra confirmed the complete sequence of acremotin B (**2**) as Ac-Trp¹-Iva²-Gln³-Aib⁴-Ile⁵-Thr⁶-Aib⁷-Leu⁸-Aib⁹-Pro¹⁰-Gln¹¹-Aib¹²-Hyp¹³-Iva¹⁴-4-mPro¹⁵-Phe¹⁶.

The positive mode HRESIMS full-scan spectra of compounds **3** and **5** displayed sodium adduct ions at m/z 1902.0156 (calcd for C₉₁H₁₃₈N₂₀O₂₃Na) and 1902.0121 (calcd for C₉₁H₁₃₈N₂₀O₂₃Na), respectively, indicating they are a pair of constitutional isomers. Moreover, a mass difference of 57 amu, likely arising from the addition of a glycine residue in the peptide backbones, was found between the [M + Na]⁺ ions of these isomers and that of acremotin A (**1**). Further investigation on the tandem HRESIMS fragmentation pattern of the sodium adduct ion of **5** revealed the presence of four intense daughter ions at m/z 864.4238 ([y₈ + Na + H]⁺), 1032.5844 ([a₉ + Na - H]⁺), 1342.7458 ([a₁₂ + Na - H]⁺) and 1554.8644 ([a₁₄ + Na - H]⁺), arising from the cleavage of three labile peptide bonds between Aib/Iva and imino acids (Table S1, Supplementary Information). The m/z of the latter three daughter ions are identical to those of sodiated a₉, a₁₂ and a₁₄ ions in **1**, respectively, while the m/z of the first daughter ion is 57 amu higher than that of [y₇ + Na + H]⁺ ion in **1**, indicating the putative glycine unit locates at the C-terminal section of **5**. Indeed, the presence of two less abundant daughter ions at m/z 1798.9902 and 1844.9912, corresponding to the [a₁₆ + Na - H]⁺ and [b₁₆ + Na + OH]⁺ ions (Table S1, Supplementary Information), suggested that instead of terminating the peptide sequence with the Phe¹⁶ as in **1**, **5** adopts an extra Gly as the C-terminal residue. Together with other fragmentation information provided by the remaining sodiated a-, b- and y-type daughter ions, the primary structure of **5** was proposed as Ac-Trp¹-Iva²-Gln³-Aib⁴-Ile⁵-Thr⁶-Aib⁷-Leu⁸-Aib⁹-Pro¹⁰-Gln¹¹-Aib¹²-Hyp¹³-Iva¹⁴-Pro¹⁵-Phe¹⁶-Gly¹⁷, and this peptide sequence was fully supported by the 1D and 2D

NMR spectroscopic data (Figure S1, Supplementary Information). Searches of this peptide sequence in the SciFinder and Peptaibiotic Database (<http://peptaibiotics-database.boku.ac.at>) gave one known peptaibiotic named XR586, which was also isolated from a tropical soil-derived strain of *Acremonium persicinum* [30].

The intense $[a_{12} + Na - H]^+$ and $[b_{16} + Na + OH]^+$ daughter ions of **3** at m/z 1342.7505 and 1844.9893, respectively, match perfectly with those of **5**, while the $[a_{14} + Na - H]^+$ ion of **3** at m/z 1540.8516 is 14 amu lower than that of **5**, suggesting the Iva¹⁴-Pro¹⁵ unit in **5** was replaced by a Aib¹⁴-4-mPro¹⁵ in **3** (Table S1, Supplementary Information). The ¹H and ¹³C NMR spectra of these two compounds showed extreme similarity, and detailed analysis of the 2D NMR spectra (Figure S1, Supplementary Information) sufficiently supported the complete sequence of **3** as Ac-Trp¹-Iva²-Gln³-Aib⁴-Ile⁵-Thr⁶-Aib⁷-Leu⁸-Aib⁹-Pro¹⁰-Gln¹¹-Aib¹²-Hyp¹³-Aib¹⁴-4-mPro¹⁵-Phe¹⁶-Gly¹⁷. Searches of this sequence in the databases confirmed **3** as a new peptaibiotic and a trivial name acremotin C was given.

The HRESIMS determined molecular weight of acremotin D (**4**), 1893.0400, is 57 amu higher than that of acremotin B (**2**). With the preceding example of **1** and **5** in hand, it is reasonable to assume that **4** is a heptadecapeptide whose first sixteen residues (starting from the N-terminus) are identical to those of **2** while the C-terminal amino acid is a glycine. This proposed primary structure of **4** was carefully examined by interpretation of HRESIMS/MS and NMR spectroscopic data. The presence of $[b_{16} + Na + OH]^+$ ion at m/z 1859.0046 in the HRESIMS/MS spectrum (Table S1, Supplementary Information) together with the HMBC correlation between the amidic proton (δ_H 7.79, m) of Gly¹⁷ and the carbonyl carbon of Phe¹⁶ (δ_C 174.7) (Figure S1, Supplementary Information) confirmed glycine as the C-terminal residue. On the basis of abovementioned evidence, the complete sequence of acremotin D (**4**) was determined as Ac-Trp¹-Iva²-Gln³-Aib⁴-Ile⁵-Thr⁶-Aib⁷-Leu⁸-Aib⁹-Pro¹⁰-Gln¹¹-Aib¹²-Hyp¹³-Iva¹⁴-4-mPro¹⁵-Phe¹⁶-Gly¹⁷.

As the most abundant peptaibiotic isolated from the fermentation broth of *Acremonium persicinum* SC0105, acremotin D (**4**) was selected to investigate the absolute configurations of each amino acid presented in **1–5**. The derivatization of amino acids was carried out using the advanced Marfey's method after acidic hydrolysis of **4**, and the resulting derivatives were analyzed by UPLC-MS. Authentic (4*R*)-4-hydroxy-L-proline and (4*S*)-4-methyl-L-proline were used as reference. The absolute configurations of all proteinogenic amino acids were determined as L, while the Hyp and 4-mPro residues presented in **4** were confirmed as (4*R*)-4-hydroxy-L-proline and (4*S*)-4-methyl-L-proline, respectively. It is noteworthy that, like many other isovaline containing peptaibiotics [31–33], **4** adopts

both D- and L-isovaline as building blocks to construct the peptide backbone. The issue regarding the specific location of D- and L-Iva residues, however, is not addressed in the present study. Since compounds **1–5** share the same biosynthetic origin, it is reasonable to assume that the absolute configurations of amino acids presented in **1–3** and **5** are same as those of **4**.

It is clear that acremotins A–D (**1–4**) belong to the peptaibiotic subfamily-3 (SF3) after aligning their sequences with those of representative members of peptaibiotic SF1 (alamethicin, chrysospermin C, etc.), SF2 (antiamoein I, emerimicin IV, etc.) and SF3 (zervamicin IIB, emerimicin IIA, XR586, etc.) (Figure S2, Supplementary Information). **1–4** inherit all characteristic structural features of SF3 peptaibiotics, including the aromatic residues (Phe and Trp) at both N- and C-termini, the imino acids (Pro, Hyp and 4-mPro) at positions 10, 13 and 15, two Glns at position 3 and 11, and the highly conserved Thr residue at position 6 [34]. Unlike the peptaibols, which adopt 2-amino alcohols as the C-terminal moiety, **1–4** terminate the peptide sequences with an unreduced Phe or Gly. The high similarity in primary sequences of acremotins A–D with zervamicins indicates acremotins A–D would likely resemble the helical structure of zervamicin IIB and [Leu¹]zervamicin [2, 35]. This speculation is supported by the CD spectrum of **4** (Fig. 4) which displays a positive band around 200 nm and negative bands at 208 nm and 230 nm, characteristic for a helical structure [36, 37]. In order to gain deeper insights into the biochemical properties of our peptaibiotics, we established the three-dimensional (3D) structure of **4** by theoretical conformational analysis using the DFT method (see Supplementary Information for computational details). As shown in Fig. 5a, the theoretical solution (MeOH) 3D structure of **4**, which is quite similar to the X-ray crystal and NMR structures of zervamicins [2, 35], is characterized as an amphiphilic helix with a bend at Pro¹⁰ (bending angle around 35°). The polar side chains of Gln³, Thr⁶ and Hyp¹³

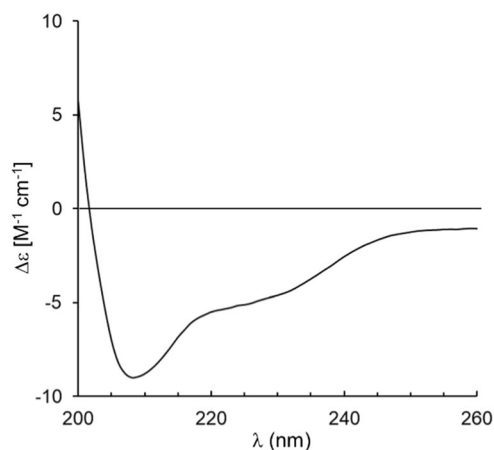


Fig. 4 CD spectrum of acremotin D (**4**) in methanol

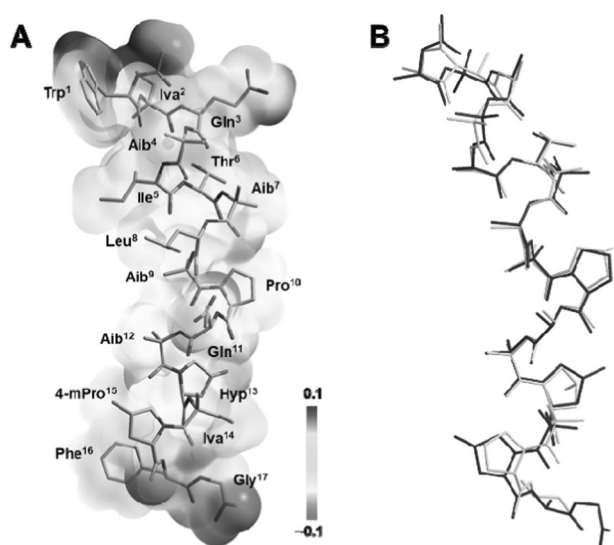


Fig. 5 Stereo diagram of acremotin D (**4**). **a** Theoretical solution 3D structure and electrostatic potential (ESP) surface of acremotin D. **b** Backbone superimposition of acremotin D (in blue) with [Leu¹]zervamicin (in yellow, CSD code: KIYPUD). For better visualization, the side chains of Trp, Phe, Leu, Ile, Gln and Iva were truncated and the omitted parts were replaced by hydrogen atoms

as well as the free COOH group of Gly¹⁷ in **4** are situated on the convex side of the banana-shaped helix, while the concave surface is constituted by bulky hydrophobic side chains of Trp¹, Ile⁵, Leu⁸, 4-mPro¹⁵ and Phe¹⁶. An α -helix is formed from the N-terminus through the Aib⁹ by virtue of the $i, i + 4$ type hydrogen bondings of Trp¹ C = O/Ile⁵ NH, Iva² C = O/Thr⁶ NH, Gln³ C = O/Aib⁷ NH, Aib⁴ C = O/Leu⁸ NH and Ile⁵ C = O/Aib⁹ NH. As for the other half of the helix, a β -ribbon accommodating Pro¹⁰, Hyp¹³ and 4-mPro¹⁵ is twisted into a helix which is stabilized by the $i, i + 3$ type hydrogen bonds of Leu⁸ C = O/Gln¹¹ NH, Aib⁹ C = O/Aib¹² NH, Gln¹¹ C = O/Iva¹⁴ NH, Hyp¹³ C = O/Phe¹⁶ NH and Iva¹⁴ C = O/Gly¹⁷ NH. This amphiphilic and helical structure of **4** is almost superimposable to the crystal structure of [Leu¹]zervamicin with minor variations occurring at the C-terminus due to the incorporation of an extra glycine residue (Fig. 5b).

Bioassays

The antibacterial and cytotoxic activity of acremotins A–D (**1–4**) and XR586 (**5**) were examined by cell-based assays. All five peptaibiotics displayed growth inhibitory activity against two gram-positive bacterial pathogens *Staphylococcus aureus* ATCC6548 and methicillin-resistant *S. aureus* (MRSA) 11646 (MIC ranging from 6.25 to 50 $\mu\text{g/ml}$), but were inactive against the gram-negative bacteria *Shigella Dysenteriae* CMCC51252, *Salmonella typhimurium* CMCC50115 and *Escherichia coli* ATCC8739 (MIC \geq 100

$\mu\text{g/ml}$) (Table 2). **4** was the most active compound among these peptaibiotics, which showed MIC of 12.5 and 6.25 $\mu\text{g/ml}$ against *S. aureus* and MRSA, respectively. **1–5** also exhibited strong to moderate cytotoxicity against three cancer cell lines, including human lung carcinoma A549 cells, human cervical carcinoma HeLa cells and human hepatocellular carcinoma HepG2 cells (IC₅₀ ranging from 1.2 to 21.6 μM) (Table 3). Among these peptaibiotics, **2** and **4** were the most cytotoxic compounds, showing IC₅₀ all below 4 μM against tested cancer cells and specifically both having an IC₅₀ of 1.2 μM against HepG2 cells. These cytotoxic peptaibiotics were also able to inhibit the growth of the African green monkey kidney Vero cells with IC₅₀ ranging from 1.7 to 8.3 μM . It is noteworthy that methylation on the γ -carbon of Pro¹⁵ increases both antibacterial and cytotoxic activity of compounds **1** and **5** (**2** vs. **1**; **4** vs. **5**), suggesting the 4-mPro¹⁵ residue is beneficial to the bioactivity of our peptaibiotics.

Experimental

General experimental procedures

Optical rotations were recorded in MeOH on a Perkin-Elmer 343 spectropolarimeter. UV spectra were measured in methanol with a Perkin Elmer Lambda 650 UV/VIS spectrometer. Infrared spectra were recorded by a SHIMADZU IRAffinity-1 spectrometer. CD spectrum of **4** in methanol was recorded on a Chirascan CD spectrometer (Applied Photophysics Ltd., England) using 50 nm/min scanning speed, 1 nm bandwidth and three accumulations. The CD spectrum of solvent methanol was used as the baseline and was subtracted from the experimental spectrum. ¹H, ¹³C and 2D NMR data were obtained on a Bruker Avance 600 instrument using the residual solvent peak as reference. High-resolution electrospray ionization mass spectrometry (HRESIMS) and CID MS/MS spectra were obtained on a Bruker maXis Q-TOF mass spectrometer in positive-ion mode (capillary voltage: 4.5 kV, end plate offset: 500 V, nebulizer: 0.4 bar, dry gas: nitrogen, dry temperature: 180 °C). For CID, high-purity nitrogen was used as buffer gas and the normalized collision energy was set as 10–100 eV. Preparative HPLC was performed on a Waters 600 pump and a 2487 dual λ absorbance detector with a Shimadzu Shim-Pack Pro-ODS column (20 mm \times 25 cm) (Shimadzu Corp., Japan). For column chromatography, Diaion HP-20 resin (Mitsubishi Chemical Corp., Japan) and YMC ODS-A (75 μm , YMC Co. Ltd., Japan) were used. Analytical TLC was performed on HSGF254 silica gel plates (0.2 mm, Yantai Jiangyou silica gel Development Co. Ltd., Yantai, China); spots were visualized after spraying with 10% H₂SO₄ solution followed by heating.

Table 2 Antibacterial activity (MIC, $\mu\text{g ml}^{-1}$) of compounds 1–5

compound	<i>S. aureus</i> ATCC 6538	MRSA 11646	<i>S. dysenteriae</i> CMCC 51252	<i>S. typhimurium</i> CMCC 50115	<i>E. coli</i> ATCC 8739
1	25	50	>100	>100	>100
2	12.5	12.5	>100	>100	100
3	12.5	25	>100	>100	>100
4	12.5	6.25	>100	>100	100
5	25	50	>100	>100	>100
kanamycin	0.78	nt	6.25	6.25	6.25
vancomycin	nt	0.78	nt	nt	nt

nt not tested

Table 3 Cytotoxic activity (IC_{50} , μM)^a of compounds 1–5

compound	cell lines			
	A549	HeLa	HepG2	Vero
1	14.4 ± 1.85	9.0 ± 1.02	4.0 ± 0.70	8.3 ± 0.20
2	2.8 ± 0.079	3.9 ± 0.28	1.2 ± 0.19	1.7 ± 0.17
3	4.0 ± 0.33	8.0 ± 1.58	1.4 ± 0.15	4.7 ± 0.52
4	2.2 ± 0.39	3.8 ± 0.63	1.2 ± 0.048	2.3 ± 0.13
5	21.6 ± 2.23	10.9 ± 0.67	4.7 ± 0.44	6.1 ± 0.85
doxorubicin	1.1 ± 0.28	0.6 ± 0.16	0.6 ± 0.16	nt

nt not tested

^aValues represent means ± SD based on three individual experiments

Producing fungus and fermentation

The producing fungus, *Acremonium persicinum* SC0105 was isolated from a humus soil sample (no. DH0011) collected in the Dinghu Mountain Biosphere Reserve, Guangdong, China in October, 2001. It was authenticated on the basis of its morphological characteristics and ITS rDNA sequence data (GenBank accession number KM086711). The culture (SC0105) is deposited at the culture collection of South Botanical Garden, Chinese Academy of Sciences, Guangzhou, China. For maintenance on agar slants and submerged cultures, the fungus was grown on PDA medium.

The mycelia of *A. persicinum* SC0105 grown on PDA plates were used to inoculate two 500 ml Erlenmeyer flasks containing 150 ml of YMG medium (glucose 0.4%, malt extract 1.0%, yeast extract 0.4%, pH 5.5). The flasks were incubated on a rotary shaker for 2 days in the dark at 25 °C with shaking at 150 rpm. Then the cultures were transferred into twenty 500 ml flasks containing 150 ml of YMG at the same incubation condition. Finally, the cultures were transferred into two hundred 500 ml flasks containing 150 ml of YMG medium and 125 g of wheat grains, and the cultivation was carried out in the stationary phase in the dark at 25 °C for 16 days.

Extraction and isolation

The obtained mycelial solid culture was extracted with 95% EtOH three times at room temperature and the combined solution was concentrated under vacuum to give the crude extract. The crude extract was dissolved in 40% aqueous methanol and subsequently subjected to Diaion HP-20 resin column chromatography, eluting with gradient aqueous methanol (methanol/water, v/v, 30/70, 80/20 and 100:0) to give three fractions (Fr. A–Fr. C). The 80% aqueous methanol eluted fraction (Fr. B) was separated by ODS column chromatography, eluting with gradient methanol (methanol/water, v/v, 40/60, 50/50, 60/40, 70/30 and 80/20) to afford five sub-fractions (Fr. B1–Fr. B5). Fr. B5 was subjected to preparative HPLC purification, using 78% aqueous methanol (with 0.1% formic acid) as mobile phase with a flow rate of 5 ml/min to yield acremotin A (**1**, t_{R} = 45 min, 10 mg), acremotin B (**2**, t_{R} = 68 min, 5 mg), acremotin C (**3**, t_{R} = 93 min, 8 mg), acremotin D (**4**, t_{R} = 60 min, 18 mg) and XR586 (**5**, t_{R} = 41 min, 7 mg).

Acremotin A (1): white powder; $[\alpha]_{\text{D}}^{20} + 9.0$ (c 0.10, CH₃OH); UV (CH₃OH) λ_{max} (log ϵ) 216 (4.60), 282 (3.67) nm; IR cm^{-1} : 3300, 2974, 2320, 1635, 1541, 1480, 1440, 1012, 646; ¹H and ¹³C NMR data see Table 1; HRESIMS m/z 1844.9846 [M + Na]⁺ (calcd for C₈₉H₁₃₅N₁₉O₂₂, 1844.9921).

Acremotin B (2): white powder; $[\alpha]_{\text{D}}^{20} + 4.6$ (c 0.17, CH₃OH); UV (CH₃OH) λ_{max} (log ϵ) 216 (4.55), 282 (3.63) nm; IR cm^{-1} : 3292, 2960, 2320, 1635, 1521, 1456, 1440, 1174, 1028, 634; ¹H and ¹³C NMR data see Table 1; HRESIMS m/z 1859.0042 [M + Na]⁺ (calcd for C₉₀H₁₃₇N₁₉O₂₂, 1859.0078).

Acremotin C (3): white powder; $[\alpha]_{\text{D}}^{20} + 3.4$ (c 0.06, CH₃OH); UV (CH₃OH) λ_{max} (log ϵ) 216 (4.60), 282 (3.71) nm; IR cm^{-1} : 3309, 2962, 2320, 1647, 1541, 1470, 1440, 1022, 600; ¹H and ¹³C NMR data see Table 1; HRESIMS m/z 1902.0156 [M + Na]⁺ (calcd for C₉₁H₁₃₈N₂₀O₂₃, 1902.0136).

Acremotin D (4): white powder; $[\alpha]_{\text{D}}^{20} + 2.1$ (c 0.58, CH₃OH); UV (CH₃OH) λ_{max} (log ϵ) 216 (4.61), 282 (3.69)

nm; IR cm^{-1} : 3292, 2962, 2320, 1635, 1531, 1417, 1286, 1176, 1022, 659; ^1H and ^{13}C NMR data see Table 1; HRESIMS m/z 1916.0198 $[\text{M} + \text{Na}]^+$ (calcd for $\text{C}_{92}\text{H}_{140}\text{N}_{20}\text{O}_{23}$, 1916.0292).

The advanced Marfey's method

The absolute configurations of each constituent amino acid (AA) in **4** were investigated using the advanced Marfey's method [38, 39] after acidic hydrolysis. In brief, compound **4** (1 mg) was hydrolyzed in 6 N HCl (1 ml) at 110 °C for 16 h in a sealed thick tube. The hydrolysate was evaporated to dryness, and the resulting residue was suspended in 100 μL acetone and equally divided into two portions. Each portion was mixed with 20 μL NaHCO_3 (1 M) and 100 μL 1-fluoro-2,4-dinitrophenyl-5-L-leucinamide or 1-fluoro-2,4-dinitrophenyl-5-DL-leucinamide (L-FDLA or DL-FDLA, 1% in acetone), respectively. The reaction mixture was heated at 45 °C for 1.5 h. After cooling to room temperature, 10 μL of 2 N HCl was added. The resulting mixture was dried and dissolved in 1 ml of 50% aqueous CH_3CN , and subsequently analyzed by UPLC-HRESIMS. UPLC runs were performed on a Waters ACQUITY UPLC I-Class system and a Waters ACQUITY UPLC[®] BEH C18 column (1.7 μm , 2.1 \times 50 mm) with a flow rate of 0.5 ml/min. Aqueous CH_3CN (with or without 0.1% formic acid) was used as mobile phase with a gradient program of 0–12 min, 20–38%; 12.1–13 min, 60%. Negative ion HRESIMS spectra were recorded on a Waters Xevo G2-XS QTOF mass spectrometer (capillary voltage: 0.43 kV, source temperature 100 °C, source offset 80, desolvation temperature 350 °C, cone gas: nitrogen at a flow rate of 50 L/h, desolvation gas: nitrogen at a flow rate of 600 L/h). Each AA-FDLA derivative was identified by the corresponding m/z value. The absolute configuration of each AA was determined by comparing the retention times of the L-FDLA derivative with those of DL-FDLA derivatives, and by applying the rules that the L-AA-L-FDLA derivatives are generally eluted faster than the D-AA-L-FDLA/L-AA-D-FDLA derivatives on the reverse phase C18 column with a few exceptions [39, 40]. See Table S2 (Supplementary Information) for the specific retention times of the AA-L-FDLA and AA-D-FDLA derivatives.

Evaluation of antibacterial activity

The Gram-positive bacteria strain *S. aureus* ATCC 6538 and three Gram-negative bacteria strains *S. dysenteriae* CMCC 51252, *S. typhimurium* CMCC 50115 and *E. coli* ATCC 8739 were purchased from the Microbial Culture Collection Center of Guangdong Institute of Microbiology (Guangzhou, China). The methicillin resistant *S. aureus* 11646 strain was kindly provided by the State Key Laboratory of Respiratory Disease, First Affiliated Hospital

of Guangzhou Medical University (Guangzhou, China). AlamarBlue[®] was obtained from Invitrogen Corporation (Carlsbad, the United States). Antibacterial activity was evaluated using the microplate AlamarBlue[®] method as previously described [41]. Briefly, each test strain was inoculated in 25 ml of Mueller Hinton Broth (MHB) (Guangdong Huankai Microbial Sci. & Tech. Co., Ltd., Guangzhou, China) and shook at 150 rpm, 37 °C for 12 h. The stock solutions (DMSO) of test compounds were diluted with DMSO to give serial two-fold dilutions. In each well of a 96-well plate, 96 μL bacterial suspension of each test strain (1×10^5 cfu/ml) containing AlamarBlue[®] (8%, v/v) was mixed with 4 μL solution of test compounds. The final concentrations of each compound in the wells were 100, 50, 25, 12.5, 6.25, 3.125, and 1.562 $\mu\text{g}/\text{ml}$. Kanamycin and vancomycin were used as positive control. The plates were incubated at 37 °C in the dark for 7 h, and the MIC value was defined as the lowest concentration of the test compound that inhibited bacterial growth.

Evaluation of cytotoxicity

Human lung carcinoma A549, human cervical carcinoma HeLa, human hepatocellular carcinoma HepG2 and American green monkey kidney Vero cell lines were purchased from Kunming Institute of Zoology, Chinese Academy of Sciences (Kunming, China). The cells were cultured in RPMI 1640 (for A549, HeLa and HepG2 cells) and DMEM (for Vero cells) medium supplemented with 10% heated-inactivated fetal bovine serum (Gibco, the United States) as well as 1% penicillin and 1% streptomycin in a 37 °C, 5% CO_2 incubator. Cell viability was assessed using the MTT method as previously described [42]. All experiments were performed in triplicate, and the data were expressed as means \pm SD of three independent experiments. Doxorubicin was used as positive control.

Acknowledgements The authors thank Ms. Aijun Sun, South China Sea Institute of Oceanology, Chinese Academy of Sciences, for HRESIMS/MS measurements. This work was supported by an NSFC grant (no. 81172942), a research project from the Bureau of Science and Technology of Guangzhou Municipality (Grant No. 201510010015), and a project from State Key Laboratory of Applied Microbiology Southern China (Grant No. SKLAM006-2015).

Compliance with ethical standards

Conflict of interest The authors declare that they have no conflict of interest.

References

1. Fox RO, Richards FM. A voltage-gated ion channel model inferred from the crystal structure of alamethicin at 1.5- Å resolution. *Nature*. 1982;300:325–30.

2. Karle L, Flippen-Anderson JL, Agarwalla S, Balaram P. Crystal structure of [Leu1] zervamicin, a membrane ion-channel peptide: Implications for gating mechanisms. *Proc Natl Acad Sci USA*. 1991;88:5307–11.
3. Sansom M, Balaram P, Karle I. Ion channel formation by zervamicin-IIB. *Eur Biophys J*. 1993;21:369–83.
4. Duchohier H. Peptaibiotics and peptaibols: an alternative to classical antibiotics? *Chem Biodivers*. 2007;4:1023–6.
5. Yun B-S, et al. Peptaivirins A and B, two new antiviral peptaibols against TMV infection. *Tetrahedron Lett*. 2000;41:1429–31.
6. Luo Y, et al. Antimicrobial peptaibols induce defense responses and systemic resistance in tobacco against tobacco mosaic virus. *FEMS Micro Lett*. 2010;313:120–6.
7. Otto A, et al. Chileno-peptins A and B, peptaibols from the Chilean *Sepedonium* aff. *chalcipori* KSH 883. *J Nat Prod*. 2016;79:929–38.
8. Ishiyama D, Satou T, Senda H, Fujimaki T, Honda R, Kanazawa S. Heptaibin, a novel antifungal peptaibol antibiotic from *Emericellopsis* sp. BAUA8289. *J Antibiot*. 2000;53:728–32.
9. He H, et al. Culicinin D, an antitumor peptaibol produced by the fungus *Culicinomyces clavisporus*, Strain LL-12I252. *J Nat Prod*. 2006;69:736–41.
10. Boot CM, et al. Four classes of structurally unusual peptides from two marine-derived fungi: Structures and bioactivities. *Tetrahedron*. 2007;63:9903–14.
11. Prasad BV, Sasisekharan V. A case study of the conformation of poly (α -aminoisobutyric acid): α -or 3_{10} -helix. *Macromolecules*. 1979;12:1107–10.
12. Paterson Y, Rumsey SM, Benedetti E, Nemethy G, Scheraga HA. Sensitivity of polypeptide conformation to geometry. Theoretical conformational analysis of oligomers of α -aminoisobutyric acid. *J Am Chem Soc*. 1981;103:2947–55.
13. Smith GD, et al. Crystal structures and conformational calculations of fragments of alamethicin containing aminoisobutyric acid. *J Am Chem Soc*. 1981;103:1493–501.
14. Marshall GR, et al. Factors governing helical preference of peptides containing multiple α,α -dialkyl amino acids. *Proc Natl Acad Sci USA*. 1990;87:487–91.
15. Degenkolb T, Berg A, Gams W, Schlegel B, Gräfe U. The occurrence of peptaibols and structurally related peptaibiotics in fungi and their mass spectrometric identification *via* diagnostic fragment ions. *J Pept Sci*. 2003;9:666–78.
16. Meyer C, Reusser F. A polypeptide antibacterial agent isolated from *Trichoderma viride*. *Cell Mol Life Sci*. 1967;23:85–86.
17. Daniel JF, Filho ER. Peptaibols of *Trichoderma*. *Nat Prod Rep*. 2007;24:1128–41.
18. McKernan PA, et al. Native calcitonin mimetics. US5698521 (1997).
19. Schiell M, et al. Cephaibols, new peptaibol antibiotics with anthelmintic properties from *Acremonium tubakii* DSM 12774. *J Antibiot*. 2001;54:220–33.
20. Degenkolb T, Heinze S, Schlegel B, Strobel G, Grafe U. Formation of new lipoaminopeptides, acremostatins A, B, and C, by co-cultivation of *Acremonium* sp. Tbp-5 and *Mycogone rosea* DSM 12973. *Biosci Biotechnol Biochem*. 2002;66:883–6.
21. Boot CM, Tenney K, Valeriote FA, Crews P. Highly N-methylated linear peptides produced by an atypical sponge-derived *Acremonium* sp. *J Nat Prod*. 2006;69:83–92.
22. Bruckner H, Becker D, Gams W, Degenkolb T. Aib and Iva in the biosphere: neither rare nor necessarily extraterrestrial. *Chem Biodivers*. 2009;6:38–56.
23. Andersson MA, et al. Acrebol, a novel toxic peptaibol produced by an *Acremonium exuviarum* indoor isolate. *J Appl Microbiol*. 2009;106:909–23.
24. Iijima M, et al. Acremo-peptin, a new peptaibol from *Acremonium* sp. PF1450. *J Antibiot*. 2017;70:791–4.
25. Wu P, et al. Bisacremines E–G, three polycyclic dimeric acremines produced by *Acremonium persicinum* SC0105. *Org Lett*. 2015;17:4922–5.
26. Wu P, Yao L, Xu L, Xue J, Wei X. Bisacremines A–D, dimeric acremines produced by a soil-derived *Acremonium persicinum* Strain. *J Nat Prod*. 2015;78:2161–6.
27. Teesch LM, Orlando RC, Adams J. Location of the alkali-metal ion in gas-phase peptide complexes. *J Am Chem Soc*. 1991;113:3668–75.
28. Lin T, Payne AH, Glish GL. Dissociation pathways of alkali-cationized peptides: opportunities for C-terminal peptide sequencing. *J Am Soc Mass Spectrom*. 2001;12:497–504.
29. Sabareesh V, Balaram P. Tandem electrospray mass spectrometric studies of proton and sodium ion adducts of neutral peptides with modified N- and C-termini: synthetic model peptides and micro-heterogeneous peptaibol antibiotics. *Rapid Commun Mass Spectrom*. 2006;20:618–28.
30. Sharman GJ, et al. Structural elucidation of XR586, a peptaibol-like antibiotic from *Acremonium persicinum*. *Biochem J*. 1996;320:723–8.
31. Chikanishi T, Hasumi K, Harada T, Kawasaki N, Endo A. Clo-nostachin, a novel peptaibol that inhibits platelet aggregation. *J Antibiot*. 1997;50:105–10.
32. Singh SB, et al. Integramides A and B, two novel non-ribosomal linear peptides containing nine $C\alpha$ -methyl amino acids produced by fungal fermentations that are inhibitors of HIV-1 integrase. *Org Lett*. 2002;4:1431–4.
33. Figueroa M, et al. Peptaibols, tetramic acid derivatives, isocoumarins, and sesquiterpenes from a *Bionectria* sp. (MSX 47401). *J Nat Prod*. 2013;76:1007–15.
34. Chugh JK, Wallace BA. Peptaibols: models for ion channels. *Biochem Soc Trans*. 2001;29:565–70.
35. Balashova T, et al. NMR structure of the channel-former zervamicin IIB in isotropic solvents. *FEBS Lett*. 2000;466:333–6.
36. Manning MC, Woody RW. Theoretical CD studies of polypeptide helices: Examination of important electronic and geometric factors. *Biopolymers*. 1991;31:569–86.
37. Toniolo C, Polese A, Formaggio F, Crisma M, Kamphuis J. Circular dichroism spectrum of a peptide 3_{10} -helix. *J Am Chem Soc*. 1996;118:2744–5.
38. Harada K, et al. A method using LC/MS for determination of absolute configuration of constituent amino acids in peptide-advanced Marfey's method. *Tetrahedron Lett*. 1995;36:1515–8.
39. Fujii K, Ikai Y, Oka H, Suzuki M, Harada K. A nonempirical method using LC/MS for determination of the absolute configuration of constituent amino acids in a peptide: Combination of Marfey's method with mass spectrometry and its practical application. *Anal Chem*. 1997;69:5146–51.
40. Fujii K, et al. A nonempirical method using LC/MS for determination of the absolute configuration of constituent amino acids in a peptide: Elucidation of limitations of Marfey's method and of its separation mechanism. *Anal Chem*. 1997;69:3346–52.
41. Fu Y, Wu P, Xue J, Wei X. Cytotoxic and antibacterial quinone sesquiterpenes from a *Myrothecium* fungus. *J Nat Prod*. 2014;77:1791–9.
42. Wang C, Wu P, Shi J-F, Jiang Z-H, Wei X-Y. Synthesis and cancer cell growth inhibitory activity of icaritin derivatives. *Eur J Med Chem*. 2015;100:139–50.